Magnetic Properties of $FeCl_2 \cdot 2H_2O$†

ALBERT NARATH
Sandia Laboratory, Albuquerque, New Mexico
(Received 22 March 1965)

The magnetic properties of $FeCl_2 \cdot 2H_2O$ have been investigated by means of single-crystal magnetic susceptibility, high-field magnetization, and proton nuclear-magnetic-resonance (nmr) measurements. A transition to an antiferromagnetic state is observed at $T_N \approx 23°K$. The magnetic susceptibility tensor in the paramagnetic state has uniaxial symmetry about an axis (α) lying in the ac plane ($\alpha = a^* + 58°$). In the range 30–100°K the measured susceptibilities follow a Curie-Weiss relation with $g_\alpha = 2.4$, $g_\beta \approx g_\gamma = 1.9$, and effective Weiss constants $\Delta_\alpha = 12°K$, $\Delta_\beta \approx \Delta_\gamma = 5°K$. The zero-field proton nmr in the ordered state consists of a single spin-spin doublet with extrapolated center frequency at 0°K $\nu_0 = 9.231 \pm 0.001$ Mc/sec. Proton nmr measurements in weak external magnetic fields at 4.0°K give four symmetry-related proton local-field directions. The magnetic susceptibility and proton nmr experiments give evidence for a magnetic structure ($P_C 2/m$) in which ferromagnetic chains, parallel to the c axis, are coupled antiferromagnetically to adjacent chains. The direction of sublattice magnetization coincides with the α axis. The magnetization behavior at 4.0°K and with $\mathbf{H} \| \alpha$ exhibits two metamagnetic transitions, $H_{c1} = 39 \pm 1$ kOe and $H_{c2} = 46 \pm 1$ kOe. The corresponding magnetic moments are $M_1 = 1.4 \pm 0.1 \mu_B$ and $M_2 = 4.25 \pm 0.05 \mu_B$. The first magnetization discontinuity is shown to result from an antiferromagnetic *intra*sublattice interaction which makes the two-sublattice zero-field configuration unstable with respect to a six-sublattice modification in sufficiently strong external fields.

I. INTRODUCTION

THE dihydrates of the iron-group halides, $MX_2 \cdot 2H_2O$ (M = Mn, Fe, Co; X = Cl, Br), form an isomorphous series of crystalline compounds which promise to provide useful information about indirect exchange interactions in transition-metal salts. In a previous report[1] (hereafter referred to as I) the results of an investigation of the magnetic properties of $CoCl_2 \cdot 2H_2O$ were presented. On the basis of single-crystal magnetic susceptibility and proton nuclear-magnetic-resonance (nmr) measurements it was shown that $CoCl_2 \cdot 2H_2O$ becomes magnetically ordered below $\sim 17.5°K$. The low-temperature phase has a two-sublattice antiferromagnetic structure with antiferromagnetic intersublattice and ferromagnetic intrasublattice exchange energies of approximately equal magnitude. In accord with its large magnetic anisotropy, $CoCl_2 \cdot 2H_2O$ exhibits metamagnetic behavior below its ordering temperature in external magnetic fields applied parallel to the direction of sublattice magnetization. However, instead of the single magnetization discontinuity which is observed in other metamagnetic systems, $CoCl_2 \cdot 2H_2O$ exhibits *two* successive discontinuities.[2–4] The first jump has been interpreted[5] to result from an antiferromagnetic *intra*sublattice exchange interaction which, in a sufficiently strong parallel field, makes the two-sublattice spin configuration unstable with respect to a collinear six-sublattice modification. At the second magnetization jump the system transforms into a saturated ferromagnetic configuration. The same unusual behavior has been observed since in antiferromagnetic $CoBr_2 \cdot 2H_2O$.[3]

The purpose of the present paper is to report on a similar study of $FeCl_2 \cdot 2H_2O$. The methods of I have been applied to the elucidation of the magnetic structure of this compound. The zero-field structure is shown to differ from that of $CoCl_2 \cdot 2H_2O$ only in the direction of sublattice magnetization. As in $CoCl_2 \cdot 2H_2O$, a large magnetic anisotropy is observed as well as the anomalous two-step metamagnetic behavior.

The crystal structure of $FeCl_2 \cdot 2H_2O$ is reviewed in Sec. II. The experimental techniques used in this investigation are described in Sec. III. The principal magnetic susceptibilities of $FeCl_2 \cdot 2H_2O$ are presented in Sec. IV. The behavior of the weak-field proton nmr in the antiferromagnetic state is discussed in Sec. V. Results of magnetization measurements in the ordered state are given in Sec. VI. Our observations are summarized in Sec. VII.

II. CRYSTAL STRUCTURE

The detailed crystal structure of $FeCl_2 \cdot 2H_2O$ has been determined recently by Morosin and Graeber[6] using x-ray diffraction techniques. The diffraction study confirmed the isomorphic nature of the Mn, Fe, and Co compounds in the $MCl_2 \cdot 2H_2O$ series as deduced originally by Neuhaus[7] on the basis of morphological studies.

The room-temperature lattice constants and atomic positions are given in Table I. The unit cell has monoclinic symmetry (space group $C2/m$) and contains two formula units. However, these are related by the lattice centering operation and are thus equivalent. The structure is characterized by parallel, polymeric iron-chlorine (-$FeCl_2$-) chains which are linked together by weak

† This work was supported by the U. S. Atomic Energy Commission.

[1] A. Narath, Phys. Rev. **136**, A766 (1964).
[2] A. Narath and D. C. Barham, Bull. Am. Phys. Soc. **9**, 112 (1964).
[3] A. Narath, J. Phys. Soc. Japan **19**, 2244 (1964).
[4] H. Kobayashi and T. Haseda, J. Phys. Soc. Japan **19**, 765 (1964).
[5] A. Narath, Phys. Letters **13**, 12 (1964).
[6] B. Morosin and E. J. Graeber, J. Chem. Phys. **42**, 898 (1965).
[7] A. Neuhaus, Z. Krist. **98**, 113 (1938).

TABLE I. Room-temperature lattice parameters and atomic coordinates of $FeCl_2 \cdot 2H_2O$.

$C2/m$: $a_0=7.355$ Å, $b_0=8.548$ Å, $c_0=3.637$ Å; $\beta=98°11'$			
Position	a	b	c
Fe	0	0	0
Cl	0.2387	0	0.5584
O	0	0.2427	0
H	0.10	0.32	0.10

hydrogen bonds. The local environment about each iron ion has monoclinic symmetry and consists of four chlorine ions, arranged in a slightly distorted square planar configuration, and two water molecules, one above and one below the iron-chlorine plane. The point-group symmetry elements of the iron position are a twofold axis which coincides with the O-Fe-O axis, and a perpendicular mirror plane which contains the chlorine ligands.

The packing of the chains is illustrated in Fig. 1. It is noteworthy that the midpoints between nearest-neighbor (intrachain) and next-nearest-neighbor (interchain) iron-pairs in this structure are centers of inversion. As a consequence, canting effects due to antisymmetric exchange terms in the spin Hamiltonian are expected to be absent. This conclusion is supported by the simple, antiparallel spin structure ($\mathbf{M} \| b$) previously found in $CoCl_2 \cdot 2H_2O$.

III. EXPERIMENTAL PROCEDURES

Samples of $FeCl_2 \cdot 2H_2O$ used in the present study were prepared from commercial reagent grade $FeCl_2 \cdot 4H_2O$. Since the tetrahydrate is the stable hydrate near room temperature, single crystals of the dihydrate were grown from a saturated aqueous solution at 75°C. The temperature was kept constant within ±0.05°C by means of a thermostated oil bath. The elevated temperature required for crystal growth made the rapid oxidation of ferrous to ferric iron by atmospheric oxygen a very serious problem. A satisfactory technique for preparing the hot, saturated solution was the following. The necessary amount of $FeCl_2 \cdot 4H_2O$ was dissolved in ~1% aqueous HCl, the resulting solution was filtered to remove insoluble contaminants, and finally a small amount of reagent-grade iron wire was added. In this way advantage was taken of the reaction $Fe + Fe^{3+} \rightarrow 2Fe^{2+}$ (in acid solution)[8] and a saturated starting solution without detectable Fe^{3+} content was readily obtained. Upon solution of the iron wire, the crystal-growth chamber was sealed with two layers of Saran-Wrap. Subsequent evaporation of water through the covering resulted in the crystallization of $FeCl_2 \cdot 2H_2O$. During the crystal-growth period (~3 weeks) only negligible oxidation of the solution occurred. The final Fe^{3+} content of our crystals is estimated at less than 1%.

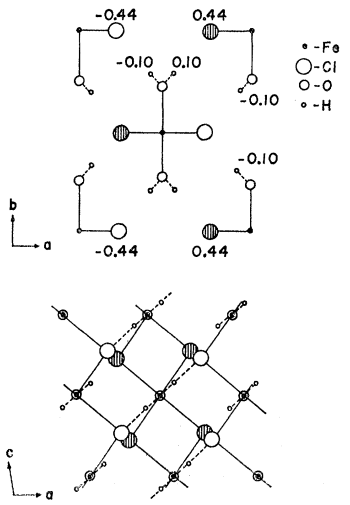

FIG. 1. Crystal structure of $FeCl_2 \cdot 2H_2O$. Top: Projection along the c axis on the ab plane. Bottom: Projection along the b axis.

The crystals prepared by the evaporation technique were always in the form of slender, prismatic needles with a preferred growth direction parallel to the crystallographic c axis. Crystals having a diameter greater than a few millimeters usually had hollow centers. In addition, most crystals were twinned on (100) planes resulting in macroscopic properties which had approximately rhombic symmetry about the crystallographic a^*, b, and c axes. The occurrence of this type of twinning was verified by x-ray diffraction measurements. This problem was eliminated by restricting measurements to very small, solid crystals (50–100 mg) which were cut from larger specimens. The results of all of our experiments were checked by measurements on several samples obtained from different crystal preparations.

The single-crystal specimens were sealed in thin Mylar for protection against moisture and oxygen, and tied to sample holders machined from phenolic plastic. The crystals were subsequently oriented by x-ray back-reflection techniques within a maximum uncertainty of 1°.

The experimental techniques for obtaining the proton nmr spectra and the temperature dependence of the ac magnetic susceptibilities were identical to those described in I.

The orientations of the principal axes of the susceptibility tensor were determined in an apparatus consisting of a small, astatic mutual inductance coil and sample assembly immersed in a liquid-nitrogen bath. The crystal mount could be rotated about an axis perpendicular to the ac field direction. Thus, the anisotropy of the susceptibility could be determined quickly at a fixed temperature of 76°K.

The apparatus for studying the 4.0°K bulk magnetization behavior of $FeCl_2 \cdot 2H_2O$ consisted of a $\frac{1}{2}$-in long multiturn coil which was mounted rigidly at the center of a 0–65 kOe superconducting solenoid and con-

[8] W. M. Latimer, *Oxidation Potentials* (Prentice-Hall, Inc., Englewood Cliffs, New Jersey, 1952), 2nd ed., p. 223.

nected to a ballistic galvanometer. The magnetic moment was related to the deflection of the galvanometer when the sample was withdrawn from the coil. The system was calibrated against the 0°K saturation moment of nickel ($0.605\mu_B$/atom).

The values of the magnetic susceptibility and magnetization reported in this paper have an estimated absolute accuracy of $\pm 5\%$.

IV. MAGNETIC SUSCEPTIBILITY

The site symmetry of the iron lattice positions is C_{2h}. Consequently, only one of the principal axis directions of the susceptibility tensor can be obtained from symmetry arguments. Thus, one of the principal axes coincides with the b axis, the other two lie in the ac plane. The orientation of the axes in this plane was determined by measurements of the susceptibility in the paramagnetic state at 76°K. Representative results of these experiments are shown in Fig. 2. These data reveal a strong magnetic anisotropy in the ac plane, similar to that detected recently in $CoCl_2 \cdot 2H_2O$.[9] Measurements of the b axis susceptibility were also carried out on the same crystals. The 76°K principal susceptibilities are

$$\begin{aligned} \chi_\alpha &= \quad 0.070 \pm 0.002 \text{ emu/mole} \\ \chi_\beta &= \quad 0.040 \pm 0.002 \text{ emu/mole} \\ \chi_\gamma &= \chi_b = 0.041 \pm 0.002 \text{ emu/mole} \\ \phi_\alpha &= +58 \pm 3^\circ, \end{aligned} \tag{1}$$

where the angle ϕ_α is defined in Fig. 3.[10] It is interesting to note that the susceptibility has uniaxial symmetry (within our experimental uncertainty) about an axis which nearly coincides with the direction of the short Fe—Cl bonds.

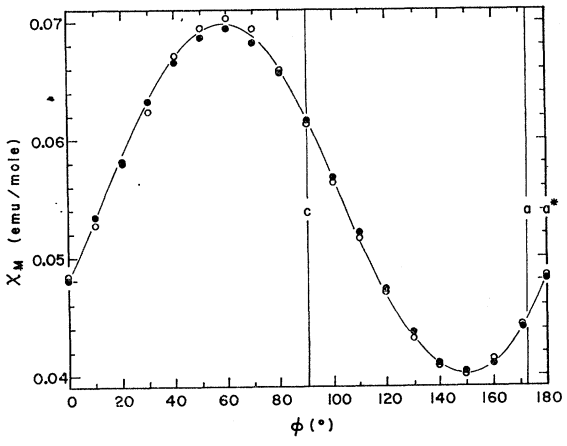

FIG. 2. Plot of the molar magnetic susceptibility of $FeCl_2 \cdot 2H_2O$ in the ac plane at 76°K for two representative untwinned single crystals.

[9] A. Narath (to be published).

[10] The 2.45 and 2.48 Å Co-Cl bond distances for $CoCl_2 \cdot 2H_2O$ in Fig. 1(a) of Ref. 1 should be interchanged.

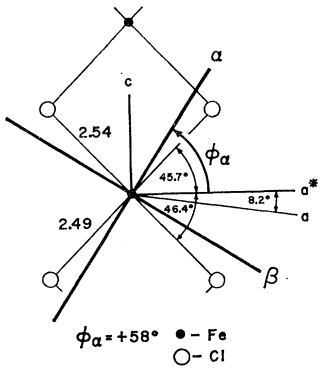

FIG. 3. Orientation of the α, β principal axes of the $FeCl_2 \cdot 2H_2O$ magnetic susceptibility tensor in the ac plane. The γ axis coincides with the crystallographic b axis.

The temperature dependence of the susceptibility was measured for the a^*, b, c, α, and β directions in the range 1–100°K. The results for the principal susceptibilities are summarized in Fig. 4. It is apparent that $FeCl_2 \cdot 2H_2O$ undergoes a magnetic transition near 23°K. The pronounced maximum in χ_α suggests that the low-temperature phase is antiferromagnetic with sublattice magnetizations directed along the α axis.

The slight rise in the susceptibilities below ~ 5°K can probably be attributed to very small occlusions of paramagnetic regions in our samples, which do not become ordered above 1°K. Since the magnitude of this effect varied among different crystals it is most likely that these paramagnetic centers are associated with Fe^{3+} contaminations.

The lowest term arising from the $(3d^6)$ configuration of the Fe^{2+} ion is ^5D. The fivefold orbital degeneracy is partially removed by an octahedral crystal field, giving an orbital triplet and a doublet. The triplet lies lowest in energy. In the presence of spin-orbit and axial crystal-field perturbations the 3×5 degeneracy of the orbital triplet is further reduced, leaving a doubly degenerate ground state. The large anisotropy of the measured susceptibility in $FeCl_2 \cdot 2H_2O$ suggests that the strength of the noncubic electrostatic perturbation is comparable to that of the spin-orbit coupling. In this case the five lowest states form an $S=2$ manifold consisting of two doublets and a singlet. The separation between these levels is a sensitive function of the relative strengths of the two perturbations. In the present case the total width of the quintet is probably not small compared to the temperatures of our experiments. In the absence of independent measurements bearing on the magnitude of the crystal-field and exchange parameters, it is not feasible to carry out a detailed analysis of the $FeCl_2 \cdot 2H_2O$ susceptibilities. We note, however, that our data in the paramagnetic range follow a Curie-Weiss relation

$$\chi_i = [N g_i^2 \mu_B^2 S(S+1)/3k(T-\Delta_i)], \tag{2}$$

where χ_i is the ith principal component of the susceptibility tensor, N is the number of paramagnetic ions, g_i is an effective g value, μ_B is the Bohr magneton, k is

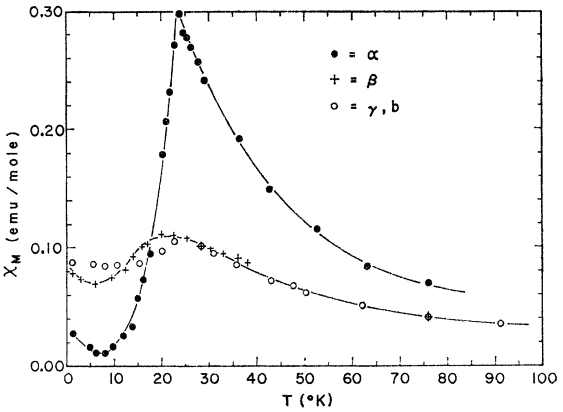

FIG. 4. Plot of the principal molar magnetic susceptibilities of $FeCl_2 \cdot 2H_2O$ as a function of temperature.

Boltzmann's constant, and Δ_i is the appropriate effective Weiss constant. The Δ_i include the effects of exchange as well as the finite width of the spin quintet. Figure 5 demonstrates the applicability of (2) to our data. Using $S=2$, one obtains from the slopes of the χ^{-1} versus T plots,

$$g_\alpha = 2.4, \quad g_\beta = g_\gamma = 1.9, \tag{3}$$

and from the intercepts,

$$\Delta_\alpha = +12°\text{K}, \quad \Delta_\beta = \Delta_\gamma = +5°\text{K}. \tag{4}$$

The corresponding plots for the a^* and c directions are also shown in Fig. 5.

V. PROTON NUCLEAR MAGNETIC RESONANCE

The nmr measurement of local-field orientations in magnetically ordered systems provides a powerful tool for examining the symmetry of the corresponding magnetic structures. Furthermore, in ideal cases a comparison between observed and calculated magnitudes of the local fields can be used to distinguish between various symmetry-allowed spin arrangements.

A search for the zero-field proton nmr in antiferromagnetic $FeCl_2 \cdot 2H_2O$ was carried out at 4.0°K in the range 5.7–25.0 Mc/sec. A single absorption was observed at 9.229 Mc/sec consisting of a spin-spin doublet with 25 kc/sec separation. (In the following discussion of the proton spectra all frequencies refer to the central frequency of the doublet.) Measurements to 1.2°K give an extrapolated 0°K proton frequency (in zero field) $\nu_0 = 9.231 \pm 0.001$ Mc/sec, corresponding to a dipole field, due to the ordered Fe^{2+} moments, of 2.168 kOe.

The observation of only one internal field greatly limits the number of possible magnetic structures for $FeCl_2 \cdot 2H_2O$. This follows from the known symmetry relations among the hydrogen positions. The two hydrogen atoms of a given water molecule are related by the twofold axis, and the two water molecules associated with each iron ion are related by reflection symmetry

The dipole field at a proton site is given by

$$H_I{}^i = \sum_j B^{ij}, \tag{5}$$

$$B^{ij} = \int_0^\infty \left(\frac{3x^i x^j - \delta_{ij} r^2}{r^5} \right) \mu_j(\mathbf{r}) d\tau, \tag{6}$$

where $H_I{}^i$ is the ith component of the dipole field and x^i, x^j $(=x, y, z)$ are the components of the vector $\mathbf{r}$ which connects a given proton site to the volume element $d\tau$ having magnetic-moment components $\mu_j(\mathbf{r})$. The requirement that the magnitude of $H_I{}^i$ be the same for all protons is satisfied in general only if the absolute values of the integrals (6) have the full crystallographic space-group symmetry of the lattice. In $FeCl_2 \cdot 2H_2O$ this requires that all protons in the magnetic unit cell be related by the operations of the magnetic space group. Therefore, the Fe^{2+} moments must lie either in the ac plane or along the b axis. Furthermore the magnetic sublattices must be collinear; i.e., the sublattices are not canted. It is reasonable, therefore, to assume that the directions of sublattice magnetization coincide with the direction of maximum g value (α axis). Furthermore, it is likely that the intrachain exchange interaction is ferromagnetic and the interchain exchange interaction is antiferromagnetic, in analogy with the $CoCl_2 \cdot 2H_2O$ magnetic structure. The resulting structure ($P_C 2/m$) for $FeCl_2 \cdot 2H_2O$ is depicted in Fig. 9(a).

In order to provide a test for the proposed structure, the directions of the internal fields at the proton positions were determined experimentally. The proton nmr was studied in weak external magnetic fields at 4.0°K. The results for rotations of a 1.000-kOe field about the b and a^* axes are shown in Figs. 6 and 7, respectively. The individual resonance diagrams have the 2π periodicity required of an antiferromagnetic structure. The observation of two resonances for the b rotation and four resonances for the a^* rotation is consistent with the symmetry of our proposed structure which predicts four symmetry-related internal-field directions.

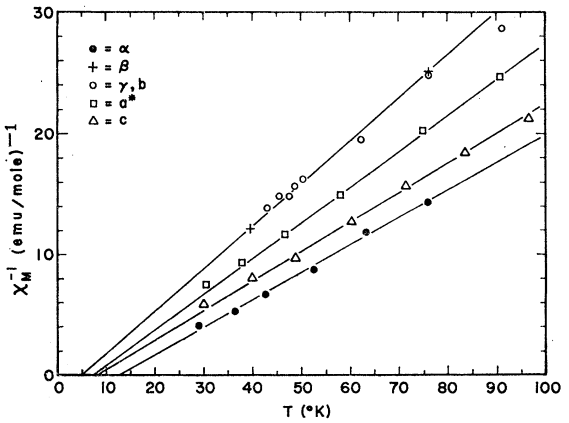

FIG. 5. Plot of reciprocal molar magnetic susceptibilities of $FeCl_2 \cdot 2H_2O$ as a function of temperature in the paramagnetic region.

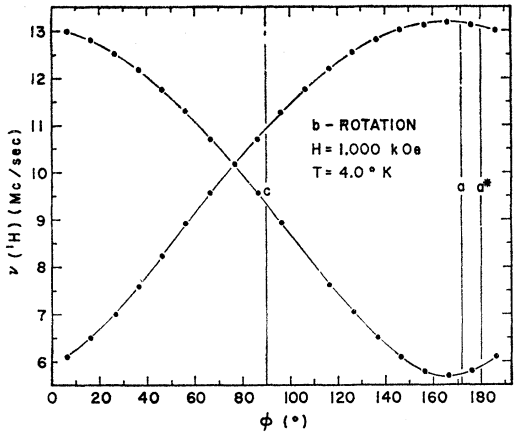

FIG. 6. Proton resonance diagram for external magnetic field directions ($H=1000$ Oe) in the ac plane of $FeCl_2 \cdot 2H_2O$ at 4.0°K.

The resonance condition is given by

$$\omega/\gamma = H_T = |(\mathbf{H}_0 + \mathbf{H}_I)|\,, \tag{7}$$

where $\omega/2\pi$ is the nmr frequency, H_T is the magnitude of the net field seen by a proton, $\mathbf{H}_0$ is the external field, and $\mathbf{H}_I$ is the internal field. The observed rotation patterns associated with the four internal-field directions are brought into agreement with (7) for the following choice of $\mathbf{H}_I$ components (ordered as indicated)

$$\begin{aligned} H_I{}^x &= (+,+,-,-)1.892 \pm 0.010 \text{ kOe} \\ H_I{}^y &= (+,-,+,-)0.955 \pm 0.010 \text{ kOe} \\ H_I{}^z &= (-,-,+,+)0.454 \pm 0.010 \text{ kOe}, \end{aligned} \tag{8}$$

where the x, y, z axes are taken to lie parallel to the crystallographic a^*, b, and c directions, respectively. The four choices of signs in (8) correspond to the four observed internal-field directions.

We have compared the measured values of $H_I{}^i$ with results of calculations based on the assumed magnetic structure, Fig. 9(a). The magnetic-moment distribution $\mu_j(\mathbf{r})$ was replaced by point dipoles situated at the iron positions. The calculation of $\mathbf{H}_I$, using (5) and (6), was carried out by direct summation (on a CDC-3600 computer) over a sufficient number of lattice points within a spherical volume to assure an accuracy of $\pm 0.1\%$ in the computed values. The magnetic moment used in the calculation was $\mu_\alpha(Fe^{2+}) = 4.25\mu_B$ as obtained from our magnetization measurements (Sec. VI).

Since the limits of error in the x-ray determination of the hydrogen positions are quite large, the geometry of the water molecule was adjusted (as in I) to conform more closely to that found in other hydrated salts. We chose the O—H bond length to be 0.97 Å and the H—O—H angle to be 108°. The hydrogen atoms were placed in the nearest neighbor Cl—O—Cl plane as determined by the x-ray measurements.

The results of our calculations, for one of the four internal-field orientations, are

$$\begin{aligned} H_I{}^x(\text{calc.}) &= +2.004 \text{ kOe} \\ H_I{}^y(\text{calc.}) &= +0.764 \text{ kOe} \\ H_I{}^z(\text{calc.}) &= +0.244 \text{ kOe}. \end{aligned} \tag{9}$$

The agreement between the observed (8) and calculated (9) values is reasonably good, although the calculated direction of the internal field is in slight disagreement with experiment. However, the direction of $\mathbf{H}_I$ is sensitive to slight changes in the geometry and orientation of the water molecule which, unfortunately, are not known accurately from the x-ray diffraction measurements. Furthermore, other magnetic structures which were examined gave much poorer agreement with experiment, as was also found in I for $CoCl_2 \cdot 2H_2O$.

From the above results it appears that the proposed magnetic structure for $FeCl_2 \cdot 2H_2O$ is in satisfactory agreement with the observed proton spectra.

VI. HIGH-FIELD MAGNETIZATION

In order to verify the predicted sublattice magnetization direction in $FeCl_2 \cdot 2H_2O$, high-field magnetization experiments were performed on untwinned single-crystal specimens at 4.0°K. These measurements were also motivated by the expectation that the large magnetic anisotropy in $FeCl_2 \cdot 2H_2O$ would lead to the two-step metamagnetic behavior observed previously in $CoCl_2 \cdot 2H_2O$ and $CoBr_2 \cdot 2H_2O$.

The results of measurements along the α, β, and γ axes are shown in Fig. 8. The two-step magnetization behavior for fields applied parallel to the α direction is clearly indicated. Two sharp transitions occur at $H_{c1} = 39 \pm 1$ kOe and $H_{c2} = 46 \pm 1$ kOe. The corresponding magnetic moments are $M_1 = 1.4 \pm 0.1\mu_B$ and $M_2 = 4.25 \pm 0.05\mu_B$. The transition regions broaden and move to higher fields for field directions (in the ac plane) which deviate slightly from the α axis. This observation

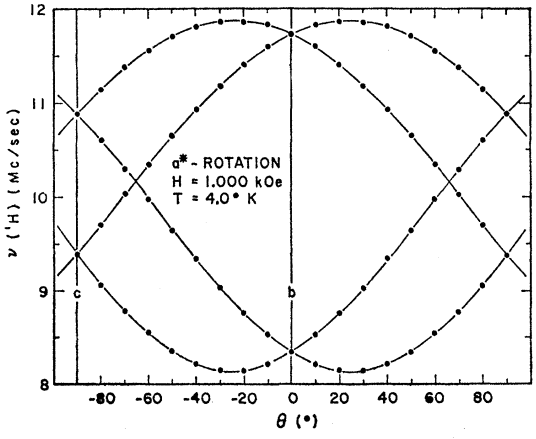

FIG. 7. Proton resonance diagram for external magnetic field directions ($H=1000$ Oe) in the bc plane of $FeCl_2 \cdot 2H_2O$ at 4.0°K.

confirms that the sublattices are indeed directed along the α axis.

The magnetization curve for $FeCl_2 \cdot 2H_2O$ in a parallel field bears a striking resemblance to the corresponding magnetization curves for $CoCl_2 \cdot 2H_2O$ and $CoBr_2 \cdot 2H_2O$. In all three cases the change in magnetic moment at the first transition is exactly $\frac{1}{2}$ of the change observed at the second transition. In $FeCl_2 \cdot 2H_2O$ the respective values are $\Delta M_1 = 1.4\mu_B$ and $\Delta M_2 = 2.8\mu_B$. The 1:3 ratio of the magnetic moments of the intermediate-field and high-field states suggests that the number of sublattices in the intermediate-field structure is a multiple of 3. The four-sublattice structure recently proposed[11] by Oguchi and Takano (O. T.) does not satisfy this requirement and predicts the wrong magnetization behavior. On the othe hand, the six-sublattice structure shown in Fig. 9(b) is in accord with the experimental data.

The single-ion ground state of Fe^{2+} in an axial crystal field is doubly degenerate. In view of the large magnetic anisotropy it is reasonable, therefore, to describe the exchange coupled spin system of $FeCl_2 \cdot 2H_2O$ in terms of Ising spins $\sigma = \frac{1}{2}$ (i.e., the spins cannot deviate from the α direction). In an external field H, parallel to the spin direction, the Hamiltonian is

$$\mathcal{H} = -\sum_{ij} J_{ij}\sigma_i^{\alpha}\sigma_j^{\alpha} - g_{\alpha}\mu_B H \sum_i \sigma_i^{\alpha}, \qquad (10)$$

where J_{ij} is an exchange constant which couples spins σ_i and σ_j. The most probable exchange interactions are the intrachain (J_0) and interchain (J_1, J_2, J_3) interactions. The latter are defined in Fig. 9(a). The intrachain interaction J_0 involves an $\sim 90°$ Fe—Cl—Fe superexchange path and is ferromagnetic. The interchain interactions J_1 and J_2 involve similar Fe—Cl—Cl—Fe

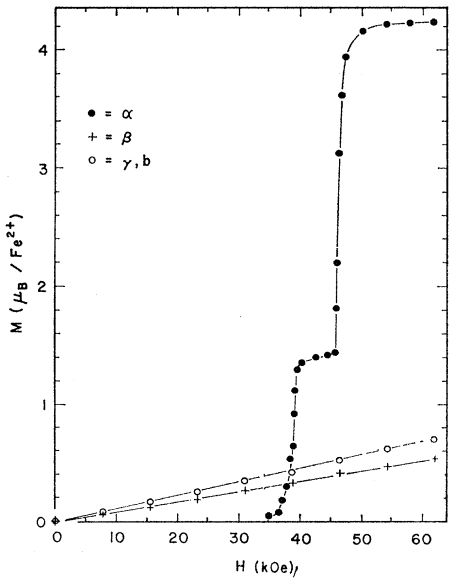

FIG. 8. Plot of the $FeCl_2 \cdot 2H_2O$ single-crystal magnetization behavior at $T = 4.0°K$.

[11] T. Oguchi and F. Takano, J. Phys. Soc. Japan **19**, 1265 (1964).

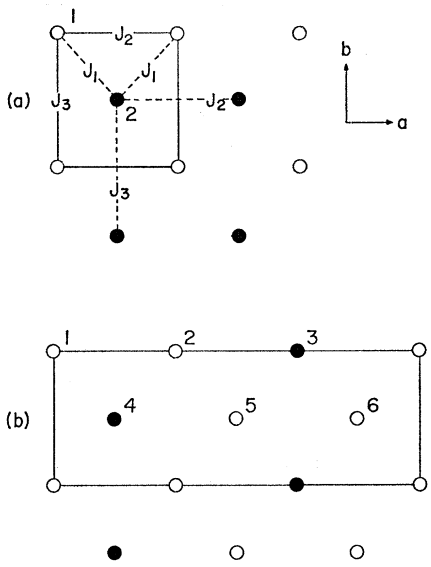

FIG. 9. Projection of $FeCl_2 \cdot 2H_2O$ spin arrangements along the c axis on the ab plane. Open circles represent spins directed along the $+\alpha$ axis and filled circles represent spins directed along the $-\alpha$ axis. (a) Zero-field, two-sublattice magnetic structure, showing the exchange paths described in the text. The numbered positions identify the sublattices. (b) Intermediate-field, six-sublattice magnetic structure in a magnetic field directed along the $+\alpha$ axis.

paths and are presumed to be antiferromagnetic. The interchain interaction J_3 couples Fe^{2+} ions which are separated by two water molecules and is, therefore, probably quite small. In terms of these interactions the 0°K energy of the two-sublattice configuration is given by

$$E_0 = -N\sigma^2(J_0 z_0 - J_1 z_1 + J_2 z_2 + J_3 z_3), \qquad (11)$$

where z_0, z_1, z_2, z_3 are the effective number of neighbors coupled to a given Fe^{2+} by the corresponding exchange interaction. The six-sublattice configuration has an energy

$$E_1 = -(N/3)\sigma^2(3J_0 z_0 - J_1 z_1 - J_2 z_2 + 3J_3 z_3) - (N/3)g_{\alpha}\mu_B \sigma H, \qquad (12)$$

and a magnetic moment $M = \frac{1}{3}M_S$, where M_S is the saturation moment. Finally, the energy of the fully saturated configuration ($M = M_S$) is given by

$$E_2 = -N\sigma^2(J_0 z_0 + J_1 z_1 + J_2 z_2 + J_3 z_3) - Ng_{\alpha}\mu_B \sigma H. \qquad (13)$$

The transition fields are therefore

$$H_{c1} = (g_{\alpha}\mu_B)^{-1}\sigma(-2J_1 z_1 + 4J_2 z_2) \qquad (14)$$

$$H_{c2} = (g_{\alpha}\mu_B)^{-1}\sigma(-2J_1 z_1 - 2J_2 z_2). \qquad (15)$$

The expressions for H_{c1} and H_{c2} were obtained from the conditions $E_0 = E_1$ and $E_1 = E_2$, respectively. Substituting the observed transition fields and making use of $g_{\alpha}\sigma = 4.25$, we find

$$FeCl_2 \cdot 2H_2O: \quad J_1 z_1/k = -24.9°K \qquad J_2 z_2/k = -\ 1.3°K. \qquad (16)$$

The corresponding values[3] for $CoCl_2 \cdot 2H_2O$ using $g_\gamma \sigma = 3.2$, $H_{c1} = 32$ kOe and $H_{c2} = 46$ kOe are

$$\begin{aligned} CoCl_2 \cdot 2H_2O: \quad & J_1 z_1/k = -17.7^\circ K \\ & J_2 z_2/k = -\ 2.1^\circ K. \end{aligned} \tag{17}$$

The number of intrachain nearest neighbors is $z_0 = 2$. The correct choice for the number of interchain neighbors in (16) and (17), however, is not clear from an examination of the structure. The nominal values are $z_1 = 4$ and $z_2 = 2$. Thus $J_1/J_2 \approx 10$ for $FeCl_2 \cdot 2H_2O$ and ≈ 4 for $CoCl_2 \cdot 2H_2O$. It is noteworthy that the magnitudes of J_1 for the two compounds are approximately in the ratio of their respective Neél temperatures.

If the third interchain constant J_3 is antiferromagnetic it must be negligibly small. This follows from the fact that the four-sublattice (O. T.) configuration[11] is not observed in our experiments. The four-sublattice structure is obtained from the zero-field structure Fig. 9(a) by reversing alternately half of the sublattice-2 spins. This configuration has an energy

$$E(\text{O.T.}) = -N\sigma^2 J_0 z_0 - (N/2) g_\alpha \mu_B \sigma H \tag{18}$$

and a magnetic moment $M = \frac{1}{2} M_S$. This configuration becomes stable relative to the six-sublattice configuration when

$$H = (g_\alpha \mu_B)^{-1} \sigma (-2J_1 z_1 - 2J_2 z_2 + 6J_3 z_3). \tag{19}$$

From a comparison of (19) with (15) it follows that a transition to this configuration should be observed if $J_3 < 0$. Thus our observations lead to the conclusion that $J_3 \gtrsim 0$.

The magnetization experiments do not give any information about the magnitude of J_0 since the ferromagnetic ordering within each chain is not disturbed by an external field. In the case of $CoCl_2 \cdot 2H_2O$ the observation of a zero Weiss constant in the paramagnetic region led to an estimate $J_0 z_0/k \approx 19^\circ K$. The corresponding value for $FeCl_2 \cdot 2H_2O$ is probably larger in view of its higher ordering temperature.

It should be emphasized that the exchange constants in (16) and (17) are based on a fictitious spin formalism. Since the true spins of Fe^{2+} and Co^{2+} at 0°K are expected to be $S_{(Fe)} \leq 2$ and $S_{(Co)} \leq 1.5$ the true exchange constants are smaller than those given in (16) and (17) by factors approaching 16 for $FeCl_2 \cdot 2H_2O$ and 9 for $CoCl_2 \cdot 2H_2O$.

From the foregoing analysis it follows that the two-step metamagnetic behavior of these compounds results from an antiferromagnetic *intra*sublattice interaction. In the limit $J_2 \geq 0$ the transformation to the saturated configuration would occur in a single step as, for example, in $FeCl_2$.[12]

[12] C. Starr, F. Bitter, and A. R. Kaufmann, Phys. Rev. **58**, 977 (1940).

Finally, we wish to remark that our interpretation of the metamagnetic properties of $FeCl_2 \cdot 2H_2O$, etc. made use of the assumption that $|J_2| > |J_3|$. If the relative magnitudes were actually reversed, a correct analysis would require a six-sublattice configuration identical to that shown in Fig. 9(b) except for an interchange of the two crystallographic directions. Furthermore, (11)–(20) remain correct if the definitions of J_2 and J_3 are also interchanged in that case. Thus our experimental observations cannot distinguish between the two possible assignments. However, the similarity of the two principal Fe—Cl—Cl—Fe exchange paths (J_1,J_2) argues strongly that $|J_2| > |J_3|$ is the correct choice.

VII. SUMMARY

An investigation of the magnetic properties of $FeCl_2 \cdot 2H_2O$ has shown that this compound becomes magnetically ordered below 23°K. In the case of $CoCl_2 \cdot 2H_2O$ the transition temperature estimated from the susceptibility maximum (17.5°K) agreed very well with the results of specific-heat measurements[13] (17.20°K). It is reasonable to assume, therefore, that the present magnetic measurements give a good estimate of the ordering temperature for $FeCl_2 \cdot 2H_2O$. This temperature is quite high for a hydrated transition metal chloride. For example, the ordering temperature[14] for the tetrahydrate ($FeCl_2 \cdot 4H_2O$) is 1.1°K. There appear to be two principal reasons for this behavior in the case of the iron and cobalt halides. First, the dihydrates have linear-chain crystal structures distinguished by an efficient *M-X-M* intrachain superexchange linkage which is ferromagnetic ($J_0 > 0$). This interaction path is similar to the intralayer exchange path found in the hexagonal layer structures of the corresponding anhydrous halides. This exchange path is missing in $FeCl_2 \cdot 4H_2O$ and $CoCl_2 \cdot 6H_2O$. Second, the ferromagnetic chains in the dihydrates are coupled by a large number of antiferromagnetic ($J_1 < 0$) *M-X-X-M* exchange paths to neighboring chains. This situation is qualitatively similar to that found in the anhydrous compounds, in which ferromagnetic layers are coupled antiferromagnetically to adjacent layers through two intervening halide layers.

The observation of two metamagnetic transformations in these compounds has provided strong evidence for the existence of an antiferromagnetic *intra*sublattice exchange interaction in this structure.

ACKNOWLEDGMENT

The author wishes to express his appreciation to Dr. B. Morosin for many stimulating discussions, and to D. C. Barham for his valuable technical assistance.

[13] H. Chihara, T. Shinoda, and S. Seki, J. Phys. Soc. Japan **19**, 1088 (1964).

[14] J. T. Schriempf and S. A. Friedberg, Phys. Rev. **136**, A518 (1964).